EHA 2026 Congress
Abstract Code: PS2460

Pharmacologic Inhibition of the Apelin Receptor (APJ) Is Protective In Murine Models of Hereditary Hemorrhagic Telangiectasia (HHT)

Jaime Darce*, Xiaofei Li*, Peter Marek, Naixin Zhang, Zach MacBain, Vasudha Sharma, Sriram Kollipara, Hitesh Soni, Arthur Marivin, Martin Marro, Anthony J. Muslin, John Diener, Peter McNamara#
*Equal contribution #Corresponding author

TECTONiC Therapeutic

Introduction

Hereditary hemorrhagic telangiectasia (HHT; Osler-Weber-Rendu syndrome) is an autosomal-dominant vascular disorder caused by loss-of-function mutations in TGF-β pathway genes, including ENG, ACVRL1/ALK1, SMAD4, and GDF2/BMP9[1]. Disruption of this pathway leads to abnormal vessel formation, mucocutaneous telangiectasias, and arteriovenous malformations (AVMs) in multiple organs, including the brain, lungs, liver, and GI tract. These fragile, tortuous vessels are prone to leakage and bleeding, often resulting in chronic anemia.

Aberrant activation of proangiogenic signaling pathways, particularly VEGF/VEGFR2, ERK and PI3K/AKT, play a central role in HHT pathogenesis and AVM formation. Genetic or pharmacologic inhibition of VEGF/VEGFR2 (impacting phosphorylation and activation of ERK and AKT) reduces hypervascularization and AVMs in multiple HHT mouse models, while direct inhibition of PI3K or AKT similarly mitigates AVM development[4-6]. These findings have led to clinical evaluation of VEGF-, PI3K-, and AKT-targeted therapies in HHT; however, systemic inhibition is associated with significant adverse effects, including hypertension and bleeding risk with VEGF blockade, and gastrointestinal toxicity, hyperglycemia, rash, and fatigue with PI3K/AKT inhibition.

Apelin is a peptide hormone that binds to and activates the G-protein coupled receptor (GPCR) apelin receptor (APJ; APLNR). APJ is mainly expressed in vascular endothelial cells where the apelin/APJ signaling pathway has a well-defined role in the promotion of angiogenesis[7]. Apelin/APJ signaling promotes endothelial cell proliferation and migration through APJ-mediated Gαi signaling, which suppresses cAMP production and contributes to increased endothelial cell permeability and barrier dysfunction[8]. In parallel, apelin/APJ activates the PI3K–AKT pathway to enhance endothelial migration and neovascularization[9]. Moreover, apelin expression is upregulated in endothelial cells across multiple genetic HHT mouse models[10]. **Accordingly, we hypothesized that inhibition of APJ signaling may restore cAMP-dependent endothelial barrier integrity while reducing PI3K–AKT–driven endothelial proliferation and migration, thus ameliorating HHT.**

AIM

Determine the contribution of the apelin/APJ signaling axis to abnormal angiogenesis and bleeding in two independent and severe HHT mouse models using a potent APJ antagonist V_{HH}-Fc molecule

Methods

In vitro signaling potency: CHOK1 cells stably expressing mouse APJ were generated using the FlpIn recombination system in FlpIn-CHOK1 parental cells. cAMP, pERK, and pAKT levels were measured with an HTRF-based method by measuring HTRF (665/620 nm) in a CLARIOstar plate reader.
Animals: All animal procedures were reviewed and approved by the Institutional Animal Care and Use Committee (IACUC) of Avastus Preclinical Services (Cambridge, MA) and conducted in compliance with its guidelines.
BMP9/10ib (BMP9/10 immunoblocked) neonatal mice model: 15mg/kg anti-BMP9 and anti-BMP10 antibodies were injected i.p. into P3 pups. Pups were sacrificed on P6, or P9. Both males and females were included. Treatment with V_{HH}-Fc isotype control (10 mg/kg), TX1351 (10 mg/kg), Akt inhibitor (Engasertib, 5 mg/kg), anti-VEGFA (G6.31, 10 mg/kg) or IgG2a/2b (as anti-BMP9/10 isotype control, 15 mg/kg) were injected i.p. at designed times.
ALK1 iKO (ALK1 inducible knockout) adult mice model: ALK1$^{f/f}$ mice and ALK1$^{f/f}$; Rosa26^{CreERT2} mice (both males and females, 8-12-month-old) were used. To induce ALK1 (*Acvrl1*) deletion, all mice were injected i.p. with tamoxifen at a dosage of 0.1 mg/g body weight at D0, and D1. The mice were administered V_{HH}-Fc control (10 mg/kg), TX1351 (10 mg/kg), or anti-VEGFA G6.31 (5 mg/kg) i.v. at D0, 3, 6, 9. Hemoglobin levels were determined with a hemoglobin photometer. At D12, all mice were euthanized. The GI hemorrhage was scored by visual inspection of the cecum.
Latex blue perfusion: To visualize blood vessels in the GI tract, mice were sequentially perfused with PBS dilator, 10% formalin, and Latex blue dye through the left ventricle chamber. The perfused GI tract was enucleated and fixed in 10% Formalin. The latex blue perfused blood vessels near Peyer's patch were imaged using a CCD camera attached to the dissection microscope. Vascular density quantification was performed using ImageJ.
Retina dissection: After the pup was euthanized, the eyes were removed. The cornea, iris, sclera, and the pigmented retina layer were removed. The lens and the vitreous humor were detached, and the inner side hyaloid vessels were removed. Four deep radial incisions were made to divide the retina into four quadrants.
Immunofluorescent staining, imaging, and analysis: The retinas were fixed, washed, and blocked with Blocking solution. The retinas were incubated with isolectin GS-IB4 Alexa Fluor 488 and rat anti-Ter119. Retinas were then washed and incubated with goat-anti-rat Alexa Fluor 594. The retinas were mounted onto slides with mount medium and coverslip. Fluorescent images for the analysis of the AVMs and bleeding area percentage were acquired by BioTek Cytation 5 imager. AVM numbers were quantified from the whole retina images by counting the direct shunts between an artery and a vein. Bleeding area percentage quantifications were analyzed using ImageJ.
RT-qPCR: RNA from retinas were isolated by RNeasy Plus mini kit. The extracted RNA concentrations were determined by Nanodrop. One-step RT-qPCR was performed by using the TaqMan™ RNA-to-CT™ 1-Step Kit on QuantStudio 7 Flex Real-Time PCR system. Data analysis was performed using the delta-delta Ct ($2^{-\Delta\Delta Ct}$) method. GAPDH served as internal control gene and fold change was calculated by normalizing all values to control.
Statistical analysis: Data are represented as mean ± SEM. Statistically significance was determined using unpaired 2-tailed student's t-test or one-way ANOVA with Tukey's multiple comparison.

Results

1. APJ antagonist shows high in vitro potency in inhibiting cAMP, p-AKT, and p-ERK

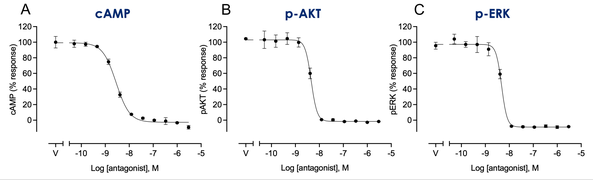

Table 1: In vitro potency of TX1351 APJ antagonist at mouse APJ

Pathway	IC_{50} Mean ± SD (n) nM
cAMP	1.6 ± 1.0 (3)
p-AKT	3.4 ± 1.2 (3)
p-ERK	3.6 ± 1.0 (3)

Figure 1: In vitro potency of TX1351 was measured using (A) cAMP, (B) p-AKT, and (C) p-ERK signaling assay with CHOK1 cells expressing mouse APJ.

2. In the neonate BMP9/10ib HHT model, TX1351 reduces AVMs and also prevents bleeding and anemia

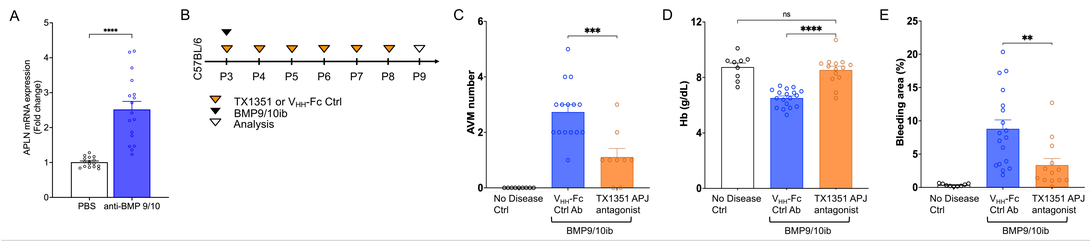

Figure 2: (A) Apelin mRNA expression in BMP9/10ib mice retinas. (B) Experimental scheme. Effects of TX1351 on (C) Retinal AVMs, (D) Hemoglobin, and (E) retinal bleeding. Data represent mean ± SEM. ** P<0.01, *** P<0.001, **** P<0.0001, unpaired 2-tailed student's t-test or one-way ANOVA with Tukey's multiple comparison.

3. AKT inhibition and VEGFA-neutralization reduce AVM formation but do not prevent anemia in the neonate BMP9/10ib HHT model

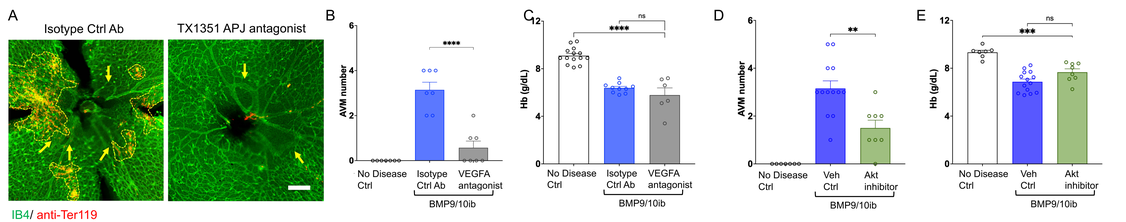

Figure 3: (A) Representative IF images of retinas from BMP9/10ib mice treated with V_{HH}-Fc isotype control, and TX1351. Yellow arrowheads indicate AVMs; yellow dashed lines outline bleeding areas. Scale bar: 200 μm. Effects of anti-VEGF treatment on (B) AVMs, and (C) Hemoglobin in BMP9/10ib neonate mice. Effects of AKT inhibitor Engasertib on (D) AVMs and (E) Hemoglobin BMP9/10ib neonate mice. Data represent mean ± SEM. ** P<0.01, *** P<0.001, **** P<0.0001, one-way ANOVA with Tukey's multiple comparison.

4. In the ALK1 iKO adult model, APJ antagonism maintains durable benefits by reducing bleeding and anemia, while anti-VEGFA effects diminish over time

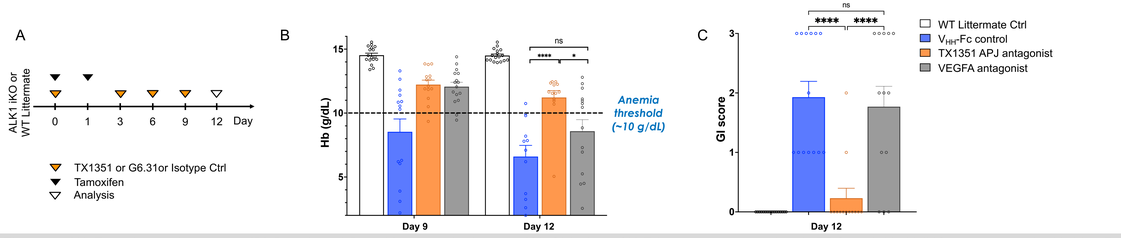

Figure 4: (A) Experimental scheme. (B) Day 9 and Day 12 Hemoglobin, and (C) GI index of WT littermates treated with PBS and ALK1 iKO mice treated with V_{HH}-Fc isotype control , TX1351, and anti-VEGFA (G6.31). Data represent mean ±SEM. * P<0.05, **** P<0.0001, ns, no significance, one-way ANOVA with Tukey's multiple comparison.

5. APJ antagonism provides more complete vascular rescue than anti-VEGFA antagonism, evidenced by significant reduction in GI hypervascularization, hemorrhage, and vein dilation in ALK1 iKO mice

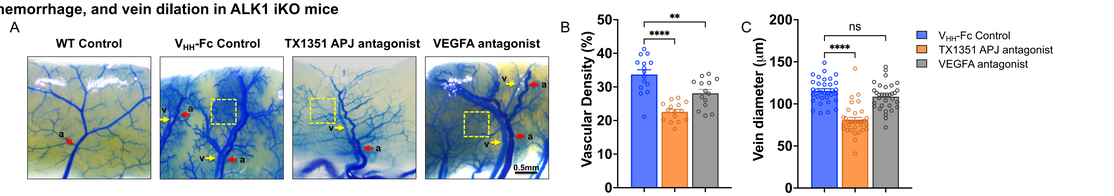

Figure 5: (A) Representative images of latex blue perfused blood vessels in small intestine near Peyer's patch from WT littermates treated with PBS and ALK1 iKO mice treated with V_{HH}-Fc isotype control, TX1351, and anti-VEGFA (G6.31). Red arrowheads: arteries. Yellow arrowheads: veins. Yellow dash line boxes: GI hemorrhage. Scale bar: 0.5 mm. (B) Vascular density, and (C) Vein diameter analysis. Data represent mean ±SEM. ** P<0.01, **** P<0.0001, ns, no significance, one-way ANOVA with Tukey's multiple comparison.

6. APJ antagonist significantly improved survival in ALK1 iKO model

Table 2: Median survival.

Groups	Median survival (Day)
WT Littermates	-
V_{HH}-Fc ctrl	15
TX1351	19
VEGFA antagonist	16

Table 3: Group Comparisons for Survival and Hazard Ratio

Groups	Survival statistics	Hazard Ratio (Logrank)
WT Littermates vs. VHH-Fc ctrl	***	0
TX1351 vs. V_{HH}-Fc ctrl	**	0.40, 95% CI [0.2, 0.9]
VEGFA antagonist vs. V_{HH}-Fc ctrl	ns	0.81, 95% CI [0.4, 1.8]

* P<0.05, ** P<0.01, *** P<0.0001, ns (no significance), n/a (not applicable). Logrank test with Holm-Šídák's multiple comparisons to determine significance between groups.

Conclusion

1. **Pharmacologic APJ inhibition Is protective in murine models of Hereditary Hemorrhagic Telangiectasia (HHT)**
2. **TX1351 is a potent APJ antagonist that inhibits Gαi induced suppression of cAMP synthesis, and both AKT and ERK phosphorylation with single nanomolar potency**
3. **TX1351 significantly reduced retinal AVM formation and bleeding in the BMP9/10ib HHT neonate model and prevented anemia, demonstrating broader therapeutic benefit than AVM reduction alone**
4. **Although VEGFA neutralization and AKT inhibition reduced retinal AVM formation, neither approach prevented anemia, suggesting that TX1351 provides additional vascular stabilization benefits in the BMP9/10ib HHT model**
5. **TX1351 reduced anemia and bleeding in the ALK1-iKO model, with APJ antagonism providing durable therapeutic benefit while anti-VEGF-mediated effects wane over time, consistent with a clinical loss in efficacy observed with patients treated with bevacizumab**
6. **APJ antagonism provides a more complete vascular rescue than VEGF antagonism, shown by a significant reduction in GI vascularization, hemorrhage and vein dilation in ALK1-iKO mice**
7. **In comparison to anti-VEGF treated animals, TX1351 significantly prolonged the survival of ALK1-iKO mice.**
8. **These pre-clinical pharmacology data suggest that APJ antagonism could have prolonged clinical benefit in HHT patients**

References

1. McDonald J, et al. Hereditary hemorrhagic telangiectasia: genetics and molecular diagnostics in a new era. *Front. Genet.* 2015; 6:1.
2. Kritharis A, et al. Hereditary hemorrhagic telangiectasia: diagnosis and management from the hematologist's perspective. *Haematologica*. 2018;103(9):1433-1443.
3. Choi EJ, et al. Enhanced responses to angiogenic cues underlie the pathogenesis of hereditary hemorrhagic telangiectasia 2. *PLoS One*. 2013;8(5):e63138.
4. Thalgott JH, et al. Decreased Expression of Vascular Endothelial Growth Factor Receptor 1 Contributes to the Pathogenesis of Hereditary Hemorrhagic Telangiectasia Type 2. *Circulation*. 2018;138(23):2698-2712.
5. Han C, et al. VEGF neutralization can prevent and normalize arteriovenous malformations in an animal model for hereditary hemorrhagic telangiectasia 2. *Angiogenesis*. 2014;17(4):823-830.
6. Ola R, et al. PI3 kinase inhibition improves vascular malformations in mouse models of hereditary haemorrhagic telangiectasia. *Nat Commun*. 2016;7:13650.
7. Wu L, et al. Apelin/APJ system: A novel promising therapy target for pathological angiogenesis. *Clin Chim Acta*. 2017;466:78-84.
8. van Nieuw Amerongen GP, et al. Targets for pharmacological intervention of endothelial hyperpermeability and barrier function. *Vascul Pharmacol*. 2002;39(4-5):257-272.
9. Gandham R, et al. Apelin and its Receptor: An Overview. *Journal of Clinical and Diagnostic Research*. 2019;13(6):BE01-BE06.
10. Zhou X, et al. ANG2 Blockade Diminishes Proangiogenic Cerebrovascular Defects Associated With Models of Hereditary Hemorrhagic Telangiectasia. *Arterioscler Thromb Vasc Biol*. 2023;43(8):1384-1403.

Acknowledgments

We extend our sincere gratitude to Tectonic Therapeutic's executive committee members, along with our investors and partners, whose generous financial support and invaluable guidance were instrumental in completing this preclinical work.

Contact Information

Tectonic Therapeutic
490 Arsenal Way Suite# 200
Watertown, MA 02474